FERMILAB-PUB-14-472-E

Measurement of the forward-backward asymmetry in the production of $B^{\pm}$ mesons in $p\bar{p}$ collisions at $\sqrt{s} = 1.96$ TeV

V.M. Abazov,[31] B. Abbott,[67] B.S. Acharya,[25] M. Adams,[46] T. Adams,[44] J.P. Agnew,[41] G.D. Alexeev,[31] G. Alkhazov,[35] A. Alton[a],[56] A. Askew,[44] S. Atkins,[54] K. Augsten,[7] C. Avila,[5] F. Badaud,[10] L. Bagby,[45] B. Baldin,[45] D.V. Bandurin,[73] S. Banerjee,[25] E. Barberis,[55] P. Baringer,[53] J.F. Bartlett,[45] U. Bassler,[15] V. Bazterra,[46] A. Bean,[53] M. Begalli,[2] L. Bellantoni,[45] S.B. Beri,[23] G. Bernardi,[14] R. Bernhard,[19] I. Bertram,[39] M. Besançon,[15] R. Beuselinck,[40] P.C. Bhat,[45] S. Bhatia,[58] V. Bhatnagar,[23] G. Blazey,[47] S. Blessing,[44] K. Bloom,[59] A. Boehnlein,[45] D. Boline,[64] E.E. Boos,[33] G. Borissov,[39] M. Borysova[l],[38] A. Brandt,[70] O. Brandt,[20] R. Brock,[57] A. Bross,[45] D. Brown,[14] X.B. Bu,[45] M. Buehler,[45] V. Buescher,[21] V. Bunichev,[33] S. Burdin[b],[39] C.P. Buszello,[37] E. Camacho-Pérez,[28] B.C.K. Casey,[45] H. Castilla-Valdez,[28] S. Caughron,[57] S. Chakrabarti,[64] K.M. Chan,[51] A. Chandra,[72] E. Chapon,[15] G. Chen,[53] S.W. Cho,[27] S. Choi,[27] B. Choudhary,[24] S. Cihangir,[45] D. Claes,[59] J. Clutter,[53] M. Cooke[k],[45] W.E. Cooper,[45] M. Corcoran,[72] F. Couderc,[15] M.-C. Cousinou,[12] D. Cutts,[69] A. Das,[42] G. Davies,[40] S.J. de Jong,[29,30] E. De La Cruz-Burelo,[28] F. Déliot,[15] R. Demina,[63] D. Denisov,[45] S.P. Denisov,[34] S. Desai,[45] C. Deterre[c],[41] K. DeVaughan,[59] H.T. Diehl,[45] M. Diesburg,[45] P.F. Ding,[41] A. Dominguez,[59] A. Dubey,[24] L.V. Dudko,[33] A. Duperrin,[12] S. Dutt,[23] M. Eads,[47] D. Edmunds,[57] J. Ellison,[43] V.D. Elvira,[45] Y. Enari,[14] H. Evans,[49] V.N. Evdokimov,[34] A. Fauré,[15] L. Feng,[47] T. Ferbel,[63] F. Fiedler,[21] F. Filthaut,[29,30] W. Fisher,[57] H.E. Fisk,[45] M. Fortner,[47] H. Fox,[39] S. Fuess,[45] P.H. Garbincius,[45] A. Garcia-Bellido,[63] J.A. García-González,[28] V. Gavrilov,[32] W. Geng,[12,57] C.E. Gerber,[46] Y. Gershtein,[60] G. Ginther,[45,63] O. Gogota,[38] G. Golovanov,[31] P.D. Grannis,[64] S. Greder,[16] H. Greenlee,[45] G. Grenier,[17] Ph. Gris,[10] J.-F. Grivaz,[13] A. Grohsjean[c],[15] S. Grünendahl,[45] M.W. Grünewald,[26] T. Guillemin,[13] G. Gutierrez,[45] P. Gutierrez,[67] J. Haley,[68] L. Han,[4] K. Harder,[41] A. Harel,[63] J.M. Hauptman,[52] J. Hays,[40] T. Head,[41] T. Hebbeker,[18] D. Hedin,[47] H. Hegab,[68] A.P. Heinson,[43] U. Heintz,[69] C. Hensel,[1] I. Heredia-De La Cruz[d],[28] K. Herner,[45] G. Hesketh[f],[41] M.D. Hildreth,[51] R. Hirosky,[73] T. Hoang,[44] J.D. Hobbs,[64] B. Hoeneisen,[9] J. Hogan,[72] M. Hohlfeld,[21] J.L. Holzbauer,[58] I. Howley,[70] Z. Hubacek,[7,15] V. Hynek,[7] I. Iashvili,[62] Y. Ilchenko,[71] R. Illingworth,[45] A.S. Ito,[45] S. Jabeen[m],[45] M. Jaffré,[13] A. Jayasinghe,[67] M.S. Jeong,[27] R. Jesik,[40] P. Jiang,[4] K. Johns,[42] E. Johnson,[57] M. Johnson,[45] A. Jonckheere,[45] P. Jonsson,[40] J. Joshi,[43] A.W. Jung,[45] A. Juste,[36] E. Kajfasz,[12] D. Karmanov,[33] I. Katsanos,[59] M. Kaur,[23] R. Kehoe,[71] S. Kermiche,[12] N. Khalatyan,[45] A. Khanov,[68] A. Kharchilava,[62] Y.N. Kharzheev,[31] I. Kiselevich,[32] J.M. Kohli,[23] A.V. Kozelov,[34] J. Kraus,[58] A. Kumar,[62] A. Kupco,[8] T. Kurča,[17] V.A. Kuzmin,[33] S. Lammers,[49] P. Lebrun,[17] H.S. Lee,[27] S.W. Lee,[52] W.M. Lee,[45] X. Lei,[42] J. Lellouch,[14] D. Li,[14] H. Li,[73] L. Li,[43] Q.Z. Li,[45] J.K. Lim,[27] D. Lincoln,[45] J. Linnemann,[57] V.V. Lipaev,[34] R. Lipton,[45] H. Liu,[71] Y. Liu,[4] A. Lobodenko,[35] M. Lokajicek,[8] R. Lopes de Sa,[45] R. Luna-Garcia[g],[28] A.L. Lyon,[45] A.K.A. Maciel,[1] R. Madar,[19] R. Magaña-Villalba,[28] S. Malik,[59] V.L. Malyshev,[31] J. Mansour,[20] J. Martínez-Ortega,[28] R. McCarthy,[64] C.L. McGivern,[41] M.M. Meijer,[29,30] A. Melnitchouk,[45] D. Menezes,[47] P.G. Mercadante,[3] M. Merkin,[33] A. Meyer,[18] J. Meyer[i],[20] F. Miconi,[16] N.K. Mondal,[25] M. Mulhearn,[73] E. Nagy,[12] M. Narain,[69] R. Nayyar,[42] H.A. Neal,[56] J.P. Negret,[5] P. Neustroev,[35] H.T. Nguyen,[73] T. Nunnemann,[22] J. Orduna,[72] N. Osman,[12] J. Osta,[51] A. Pal,[70] N. Parashar,[50] V. Parihar,[69] S.K. Park,[27] R. Partridge[e],[69] N. Parua,[49] A. Patwa[j],[65] B. Penning,[45] M. Perfilov,[33] Y. Peters,[41] K. Petridis,[41] G. Petrillo,[63] P. Pétroff,[13] M.-A. Pleier,[65] V.M. Podstavkov,[45] A.V. Popov,[34] M. Prewitt,[72] D. Price,[41] N. Prokopenko,[34] J. Qian,[56] A. Quadt,[20] B. Quinn,[58] P.N. Ratoff,[39] I. Razumov,[34] I. Ripp-Baudot,[16] F. Rizatdinova,[68] M. Rominsky,[45] A. Ross,[39] C. Royon,[15] P. Rubinov,[45] R. Ruchti,[51] G. Sajot,[11] A. Sánchez-Hernández,[28] M.P. Sanders,[22] A.S. Santos[h],[1] G. Savage,[45] M. Savitskyi,[38] L. Sawyer,[54] T. Scanlon,[40] R.D. Schamberger,[64] Y. Scheglov,[35] H. Schellman,[48] C. Schwanenberger,[41] R. Schwienhorst,[57] J. Sekaric,[53] H. Severini,[67] E. Shabalina,[20] V. Shary,[15] S. Shaw,[41] A.A. Shchukin,[34] V. Simak,[7] P. Skubic,[67] P. Slattery,[63] D. Smirnov,[51] G.R. Snow,[59] J. Snow,[66] S. Snyder,[65] S. Söldner-Rembold,[41] L. Sonnenschein,[18] K. Soustruznik,[6] J. Stark,[11] D.A. Stoyanova,[34] M. Strauss,[67] L. Suter,[41] P. Svoisky,[67] M. Titov,[15] V.V. Tokmenin,[31] Y.-T. Tsai,[63] D. Tsybychev,[64] B. Tuchming,[15] C. Tully,[61] L. Uvarov,[35] S. Uvarov,[35] S. Uzunyan,[47] R. Van Kooten,[49] W.M. van Leeuwen,[29] N. Varelas,[46] E.W. Varnes,[42] I.A. Vasilyev,[34] A.Y. Verkheev,[31] L.S. Vertogradov,[31] M. Verzocchi,[45] M. Vesterinen,[41] D. Vilanova,[15] P. Vokac,[7] H.D. Wahl,[44] M.H.L.S. Wang,[45] J. Warchol,[51] G. Watts,[74] M. Wayne,[51] J. Weichert,[21] L. Welty-Rieger,[48]

Operated by Fermi Research Alliance, LLC under Contract No. De-AC02-07CH11359 with the United States Department of Energy.

M.R.J. Williams[n],[49] G.W. Wilson,[53] M. Wobisch,[54] D.R. Wood,[55] T.R. Wyatt,[41] Y. Xie,[45] R. Yamada,[45]
S. Yang,[4] T. Yasuda,[45] Y.A. Yatsunenko,[31] W. Ye,[64] Z. Ye,[45] H. Yin,[45] K. Yip,[65] S.W. Youn,[45] J.M. Yu,[56]
J. Zennamo,[62] T.G. Zhao,[41] B. Zhou,[56] J. Zhu,[56] M. Zielinski,[63] D. Zieminska,[49] and L. Zivkovic[14]
(The D0 Collaboration[*])

[1]*LAFEX, Centro Brasileiro de Pesquisas Físicas, Rio de Janeiro, Brazil*
[2]*Universidade do Estado do Rio de Janeiro, Rio de Janeiro, Brazil*
[3]*Universidade Federal do ABC, Santo André, Brazil*
[4]*University of Science and Technology of China, Hefei, People's Republic of China*
[5]*Universidad de los Andes, Bogotá, Colombia*
[6]*Charles University, Faculty of Mathematics and Physics,*
Center for Particle Physics, Prague, Czech Republic
[7]*Czech Technical University in Prague, Prague, Czech Republic*
[8]*Institute of Physics, Academy of Sciences of the Czech Republic, Prague, Czech Republic*
[9]*Universidad San Francisco de Quito, Quito, Ecuador*
[10]*LPC, Université Blaise Pascal, CNRS/IN2P3, Clermont, France*
[11]*LPSC, Université Joseph Fourier Grenoble 1, CNRS/IN2P3,*
Institut National Polytechnique de Grenoble, Grenoble, France
[12]*CPPM, Aix-Marseille Université, CNRS/IN2P3, Marseille, France*
[13]*LAL, Université Paris-Sud, CNRS/IN2P3, Orsay, France*
[14]*LPNHE, Universités Paris VI and VII, CNRS/IN2P3, Paris, France*
[15]*CEA, Irfu, SPP, Saclay, France*
[16]*IPHC, Université de Strasbourg, CNRS/IN2P3, Strasbourg, France*
[17]*IPNL, Université Lyon 1, CNRS/IN2P3, Villeurbanne, France and Université de Lyon, Lyon, France*
[18]*III. Physikalisches Institut A, RWTH Aachen University, Aachen, Germany*
[19]*Physikalisches Institut, Universität Freiburg, Freiburg, Germany*
[20]*II. Physikalisches Institut, Georg-August-Universität Göttingen, Göttingen, Germany*
[21]*Institut für Physik, Universität Mainz, Mainz, Germany*
[22]*Ludwig-Maximilians-Universität München, München, Germany*
[23]*Panjab University, Chandigarh, India*
[24]*Delhi University, Delhi, India*
[25]*Tata Institute of Fundamental Research, Mumbai, India*
[26]*University College Dublin, Dublin, Ireland*
[27]*Korea Detector Laboratory, Korea University, Seoul, Korea*
[28]*CINVESTAV, Mexico City, Mexico*
[29]*Nikhef, Science Park, Amsterdam, the Netherlands*
[30]*Radboud University Nijmegen, Nijmegen, the Netherlands*
[31]*Joint Institute for Nuclear Research, Dubna, Russia*
[32]*Institute for Theoretical and Experimental Physics, Moscow, Russia*
[33]*Moscow State University, Moscow, Russia*
[34]*Institute for High Energy Physics, Protvino, Russia*
[35]*Petersburg Nuclear Physics Institute, St. Petersburg, Russia*
[36]*Institució Catalana de Recerca i Estudis Avançats (ICREA) and Institut de Física d'Altes Energies (IFAE), Barcelona, Spain*
[37]*Uppsala University, Uppsala, Sweden*
[38]*Taras Shevchenko National University of Kyiv, Kiev, Ukraine*
[39]*Lancaster University, Lancaster LA1 4YB, United Kingdom*
[40]*Imperial College London, London SW7 2AZ, United Kingdom*
[41]*The University of Manchester, Manchester M13 9PL, United Kingdom*
[42]*University of Arizona, Tucson, Arizona 85721, USA*
[43]*University of California Riverside, Riverside, California 92521, USA*
[44]*Florida State University, Tallahassee, Florida 32306, USA*
[45]*Fermi National Accelerator Laboratory, Batavia, Illinois 60510, USA*
[46]*University of Illinois at Chicago, Chicago, Illinois 60607, USA*
[47]*Northern Illinois University, DeKalb, Illinois 60115, USA*
[48]*Northwestern University, Evanston, Illinois 60208, USA*
[49]*Indiana University, Bloomington, Indiana 47405, USA*
[50]*Purdue University Calumet, Hammond, Indiana 46323, USA*
[51]*University of Notre Dame, Notre Dame, Indiana 46556, USA*
[52]*Iowa State University, Ames, Iowa 50011, USA*
[53]*University of Kansas, Lawrence, Kansas 66045, USA*
[54]*Louisiana Tech University, Ruston, Louisiana 71272, USA*
[55]*Northeastern University, Boston, Massachusetts 02115, USA*
[56]*University of Michigan, Ann Arbor, Michigan 48109, USA*

[57]*Michigan State University, East Lansing, Michigan 48824, USA*
[58]*University of Mississippi, University, Mississippi 38677, USA*
[59]*University of Nebraska, Lincoln, Nebraska 68588, USA*
[60]*Rutgers University, Piscataway, New Jersey 08855, USA*
[61]*Princeton University, Princeton, New Jersey 08544, USA*
[62]*State University of New York, Buffalo, New York 14260, USA*
[63]*University of Rochester, Rochester, New York 14627, USA*
[64]*State University of New York, Stony Brook, New York 11794, USA*
[65]*Brookhaven National Laboratory, Upton, New York 11973, USA*
[66]*Langston University, Langston, Oklahoma 73050, USA*
[67]*University of Oklahoma, Norman, Oklahoma 73019, USA*
[68]*Oklahoma State University, Stillwater, Oklahoma 74078, USA*
[69]*Brown University, Providence, Rhode Island 02912, USA*
[70]*University of Texas, Arlington, Texas 76019, USA*
[71]*Southern Methodist University, Dallas, Texas 75275, USA*
[72]*Rice University, Houston, Texas 77005, USA*
[73]*University of Virginia, Charlottesville, Virginia 22904, USA*
[74]*University of Washington, Seattle, Washington 98195, USA*

(Dated: November 11, 2014)

We present a measurement of the forward-backward asymmetry in the production of $B^{\pm}$ mesons, $A_{\mathrm{FB}}(B^{\pm})$, using $B^{\pm} \to J/\psi K^{\pm}$ decays in 10.4 fb^{-1} of $p\bar{p}$ collisions at $\sqrt{s} = 1.96$ TeV collected by the D0 experiment during Run II of the Tevatron collider. A non-zero asymmetry would indicate a preference for a particular flavor, i.e., b quark or $\bar{b}$ anti-quark, to be produced in the direction of the proton beam. We extract $A_{\mathrm{FB}}(B^{\pm})$ from a maximum likelihood fit to the difference between forward- and backward-produced $B^{\pm}$ mesons. We measure an asymmetry consistent with zero: $A_{\mathrm{FB}}(B^{\pm}) = [-0.24 \pm 0.41\,(\mathrm{stat}) \pm 0.19\,(\mathrm{syst})]\%$.

PACS numbers: 13.25.Hw, 11.30.Er

Over the past years there has been much interest in the forward-backward asymmetry in $t\bar{t}$ production ($A_{\mathrm{FB}}^{t\bar{t}}$) [1], especially since initial experimental results were larger than standard model (SM) predictions [2, 3]. These observations prompted development of models beyond the SM that could explain the excess [4]. The corresponding asymmetry in $b\bar{b}$ production, $A_{\mathrm{FB}}^{b\bar{b}}$, has the same sources as $A_{\mathrm{FB}}^{t\bar{t}}$ but is expected to have a smaller magnitude in the SM, making it an important probe of these new physics models [5, 6].

The most recent D0 measurements of $A_{\mathrm{FB}}^{t\bar{t}}$ [7] agree with the SM [8]. A related but smaller asymmetry has been studied at the LHC [9, 10]. The LHCb collaboration has recently measured $A_{\mathrm{FB}}^{b\bar{b}}$ in pp collisions as a charge asymmetry between b and $\bar{b}$ jets of $[0.4 \pm 0.4\,(\mathrm{stat}) \pm 0.3\,(\mathrm{syst})]\%$, for the mass range $40 < M(b\bar{b}) < 75$ GeV [11].

A forward-backward asymmetry in the production of heavy quark Q is primarily caused by interference between tree-level and loop diagrams for $q\bar{q} \to Q\bar{Q}$ interactions, and also by interference between initial and final state gluon radiation [12]. We measure the forward-backward asymmetry using fully reconstructed $B^{\pm} \to J/\psi(\to \mu^{+}\mu^{-})K^{\pm}$ decays where the $B^{\pm}$ directly identifies the quark flavor (i.e., b or $\bar{b}$). This method is unique since there is no need to account for particle-antiparticle oscillations present in neutral B mesons. The quantity $A_{\mathrm{FB}}(B^{\pm})$ is sensitive to the same production asymmetries as $A_{\mathrm{FB}}^{b\bar{b}}$. In $p\bar{p}$ collisions, the forward category indicates a $b\,(\bar{b})$ quark, or $B^{-}\,(B^{+})$ meson, emitted with longitudinal momentum component in the direction of the proton (antiproton) beam.

We reconstruct a $B^{\pm}$ meson and categorize it as forward or backward with a variable $q_{\mathrm{FB}} = -q_B\,\mathrm{sgn}(\eta_B)$, where q_B is the $B^{\pm}$ meson electric charge, $\mathrm{sgn}(x)$ is the sign function, and η_B is the $B^{\pm}$ meson pseudorapidity [13]. The forward-backward asymmetry of the $B^{\pm}$ mesons is:

$$A_{\mathrm{FB}}(B^{\pm}) = \frac{N(q_{\mathrm{FB}} > 0) - N(q_{\mathrm{FB}} < 0)}{N(q_{\mathrm{FB}} > 0) + N(q_{\mathrm{FB}} < 0)}. \quad (1)$$

Inclusive predictions of $A_{\mathrm{FB}}^{b\bar{b}}$ give positive asymmetries of $\approx 0.5\%$ [5, 14], but the mass scales of the $b\bar{b}$ pairs considered ($M(b\bar{b}) > 35$ GeV, or $p(b) > \approx 15$ GeV) are more

---

[*] with visitors from [a]Augustana College, Sioux Falls, SD, USA, [b]The University of Liverpool, Liverpool, UK, [c]DESY, Hamburg, Germany, [d]Universidad Michoacana de San Nicolas de Hidalgo, Morelia, Mexico [e]SLAC, Menlo Park, CA, USA, [f]University College London, London, UK, [g]Centro de Investigacion en Computacion - IPN, Mexico City, Mexico, [h]Universidade Estadual Paulista, São Paulo, Brazil, [i]Karlsruher Institut für Technologie (KIT) - Steinbuch Centre for Computing (SCC), D-76128 Karlsruhe, Germany, [j]Office of Science, U.S. Department of Energy, Washington, D.C. 20585, USA, [k]American Association for the Advancement of Science, Washington, D.C. 20005, USA, [l]Kiev Institute for Nuclear Research, Kiev, Ukraine, [m]University of Maryland, College Park, Maryland 20742, USA and [n]European Orgnaization for Nuclear Research (CERN), Geneva, Switzerland

relevant for a jet-based analysis. To make SM predictions tailored to our kinematics and selections, we produce next-to-leading-order Monte Carlo (MC) samples for QCD production of $B^{\pm}$ in the process $p\bar{p} \rightarrow b\bar{b}X$. MC events are generated using MC@NLO [15] with parton distribution function (PDF) set CTEQ6M1 [16] and HERWIG [17] for parton showering and hadronization. Detector simulation is performed using GEANT3 [18].

The D0 experiment collected data at $\sqrt{s} = 1.96$ TeV during Run II of the Fermilab Tevatron $p\bar{p}$ collider, from 2002 through the Tevatron shutdown in 2011. The D0 detector is described in detail elsewhere [19]. For this analysis the most important detector elements are the central tracking and muon systems. The central tracking system consists of a silicon microstrip tracker and a central fiber tracker, both located within a 1.9 T superconducting solenoidal magnet, with designs optimized for tracking and vertex finding at pseudorapidities $|\eta| < 3$ and $|\eta| < 2.5$, respectively. The muon system has a layer of tracking detectors and scintillation trigger counters outside a liquid argon sampling calorimeter and two similar layers outside a 1.8 T iron toroid [20], and covers the region $|\eta_{\rm det}| \approx 2$ where $|\eta_{\rm det}|$ is measured from the center of the detector. The solenoid and toroid magnet polarities were reversed approximately every two weeks giving nearly equal beam exposure to each polarity combination. The data used in this analysis were collected with a suite of single muon and dimuon triggers.

Events containing $B^{\pm} \rightarrow J/\psi K^{\pm}$ candidates are selected from the D0 Run II dataset with an integrated luminosity of 10.4 fb^{-1}. Candidates are reconstructed by identifying a pair of oppositely charged muons (decay products of the J/ψ meson) that are produced along with a charged track (the $K^{\pm}$ candidate) at a common vertex displaced from the $p\bar{p}$ interaction vertex.

All tracks must lie within the pseudorapidity coverage of the muon and central tracking systems, $|\eta| < 2.1$. Selected muons have transverse momentum $p_T > 1.5$ GeV, and $K^{\pm}$ candidates have $p_T > 0.7$ GeV. At least one muon must traverse both inner and outer layers of the muon detector. Both muons must match to tracks in the central tracking system. The J/ψ candidates with reconstructed invariant mass $M(\mu^+\mu^-)$ between 2.7 and 3.45 GeV are accepted if their transverse decay length (L_{xy}) uncertainty is less than 0.1 cm, where L_{xy} is the distance from the $p\bar{p}$ vertex to a particle's decay vertex in the x-y plane. The cosine of the pointing angle [21] must be greater than zero.

The combination of μ^+, μ^-, and $K^{\pm}$ tracks to form a $B^{\pm}$ decay vertex must have $\chi^2 < 16$ for three degrees of freedom, and the cosine of the $B^{\pm}$ pointing angle must be above 0.8. $B^{\pm}$ candidates are accepted if they are significantly displaced from the $p\bar{p}$ vertex. Their transverse decay length significance (defined as L_{xy} divided by its uncertainty) must be greater than three. To calculate the $B^{\pm}$ candidate mass we correct the muon momenta by constraining $M(\mu^+\mu^-)$ to the world average J/ψ meson mass [22]. The selected $B^{\pm}$ mass range is 5.05 – 5.65 GeV.

Because definitions of forward and backward are tied directly to sgn(η_B), the ambiguous region near $\eta_B = 0$ is given special consideration. We compare η of the $B^{\pm}$ mesons and their parent b quarks at production and reconstruction level in MC@NLO. Rejecting events with $|\eta_B| < 0.1$ removes all $B^{\pm}$ mesons reconstructed with incorrect $q_{\rm FB}$ without significantly affecting $A_{\rm FB}(B^{\pm})$. After the cut, more than 99.95% of $B^{\pm}$ mesons give the same $q_{\rm FB}$ as the parent b quark, indicating minimal hadronization effects on $A_{\rm FB}(B^{\pm})$. The distribution of $(\eta_b - \eta_B)$ has an RMS width of 0.06.

Background rejection is improved using a boosted decision tree (BDT) [23] trained on simulated MC signal and background from data sidebands above and below the selected $B^{\pm}$ mass range (4.0 − 5.05 and 5.65 − 7.0 GeV). Leading-order signal MC events are generated with PYTHIA [24] and processed through the same reconstruction code used for data. We weight MC events so that the p_T distributions of the muons match the distributions in data, which are affected by trigger efficiency. Additional weights are applied to match distributions of $p_T(B^{\pm})$, $p_T(K^{\pm})$, and χ^2 of the $B^{\pm}$ decay vertex fit to data distributions. Finally, we weight MC events so that the probability of reconstructing isolated muons or $B^{\pm}$ candidates matches the probability in data. Isolated particles have no other tracks in a cone of size $\Delta\mathcal{R} = 1$ around them, where $\Delta\mathcal{R} = \sqrt{\Delta\phi^2 + \Delta\eta^2}$ is the angular separation between tracks. This weighting gives optimal agreement between data and simulation in all 40 BDT input variables, which include particle momenta, distances from the $p\bar{p}$ vertex, decay lengths, pointing angles, isolation of the muons and $B^{\pm}$ meson, and azimuthal angle separation for various particle pairs. A cut on the BDT discriminant is chosen to minimize the statistical uncertainty of $A_{\rm FB}(B^{\pm})$. After all cuts we find one $B^{\pm}$ candidate in 98.5% of events, with the remainder having two or more candidates. All candidates are used independently in this analysis.

We extract $A_{\rm FB}(B^{\pm})$ from a maximum likelihood fit incorporating a signal probability distribution and three background distributions (see below), which are functions of the reconstructed $B^{\pm}$ mass $m_{J/\psi K}$ and the kaon energy E_K. The signal distribution $S(m_{J/\psi K}, E_K)$ is modeled by a double-Gaussian function with six parameters, where both Gaussians have the same mean but different widths. The widths have an exponential dependence on E_K. Signal parameters are allowed to differ for the $\eta < -0.1$ and $\eta > 0.1$ regions to account for slight differences in the magnetic field along the beam direction.

The background distribution $P(m_{J/\psi K}, E_K)$ describes $B^{\pm} \rightarrow J/\psi\pi^{\pm}$ events where the pion is assigned the kaon mass, creating an artificially high reconstructed $B^{\pm}$ mass. Distribution P is a reflection of S with the mean mass value shifted to account for the K/π mass difference and the widths scaled by a ratio of the mean mass values. Background distribution $T(m_{J/\psi K})$ describes partially reconstructed decays of type $B_x \to J/\psi h^\pm X$, which have reconstructed mass lower than the $B^\pm$ mass. Distribution T is empirically modeled using a threshold function with a floating inflection point and the slope fixed from MC simulation [25, 26]. Finally, the background distribution $E(m_{J/\psi K}, E_K)$ describes combinatoric background and is modeled using an exponential function with three parameters, where the slope depends on E_K.

The unbinned fit minimizes LLH, the negative log of the likelihood function $\mathcal{L}_n$ summed over N selected $B^\pm$ candidates, each with weight w_n (defined below):

$$\text{LLH} = -2\sum_{n=1}^{N} w_n \ln(\mathcal{L}_n). \tag{2}$$

Here $\mathcal{L}_n$ is a function of the four probability density distributions, with each distribution assigned sample fraction f_i and forward-backward asymmetry A_i. The likelihood $\mathcal{L}_n$ has 26 parameters and is normalized to 1:

$$\begin{aligned}\mathcal{L}_n = \alpha(E_K)[f_S(1+q_{\text{FB}}A_S)S + f_P(1+q_{\text{FB}}A_P)P \\ + f_T(1+q_{\text{FB}}A_T)T] + f_E(1+q_{\text{FB}}A_E)E,\end{aligned} \tag{3}$$

where $f_E = [1-\alpha(E_K)(f_S+f_P+f_T)]$ and $\alpha(E_K)$ uses three parameters to describe the dependence of the sample fractions on E_K [25].

Asymmetries in detector material and in J/ψ or $K^\pm$ reconstruction between $\eta < 0$ (the "north" side of the detector) and $\eta > 0$ (the "south" side) can result in apparent A_{FB}. A north-south asymmetry is defined as $A_{\text{NS}} = (N_N - N_S)/(N_N + N_S)$. Because B^+ and B^- particles on the same side of the detector have opposite q_{FB}, north-south efficiency corrections will generally cancel when determining $A_{\text{FB}}(B^\pm)$. We measure A_{NS} in data samples with no expected production asymmetries. Decays of $\phi \to K^+K^-$ are used to measure $A_{\text{NS}}(K^\pm)$. Signal and background models are determined from MC simulation and a χ^2 minimization fit is performed simultaneously on north- and south-side data. We meaure $A_{\text{NS}}(K^\pm)$ in bins of leading kaon $|\eta|$; there is no significant dependence on p_T. Integrated over all $|\eta|$, $A_{\text{NS}}(K^+)$ = $(0.39 \pm 0.22)\%$ and $A_{\text{NS}}(K^-) = (0.64 \pm 0.23)\%$.

Prompt $J/\psi \to \mu^+\mu^-$ decays are used to measure $A_{\text{NS}}(J/\psi)$. J/ψ mesons with significant L_{xy} are generally from B decays which could exhibit a north-south asymmetry due to $A_{\text{FB}}(B^\pm)$. To reduce the fraction of non-prompt J/ψ mesons we require the J/ψ L_{xy} significance to be less than 1.5. Background events under the peak from 2.9 − 3.3 GeV are removed with a sideband subtraction, and $A_{\text{NS}}(J/\psi)$ is calculated in bins of $|\eta|$ and p_T. Integrated over all $|\eta|$ and p_T, $A_{\text{NS}}(J/\psi) = (-0.41 \pm 0.04)\%$.

Measured A_{NS} values are used to determine "efficiency weights" $w_{K^\pm}$ and $w_{J/\psi}$ that equalize the relative reconstruction efficiencies on both sides of the detector. Applying these weights has a small effect on $A_{\text{FB}}(B^\pm)$: a shift of 0.06% from $w_{K^\pm}$ and a shift of −0.01% from $w_{J/\psi}$. Uncertainties on $A_{\text{NS}}(J/\psi)$ and $A_{\text{NS}}(K^\pm)$ contribute an uncertainty of 0.003% to $A_{\text{FB}}(B^\pm)$, determined using an ensemble test with 500 Gaussian variations of the A_{NS} values.

The total event weight is $w_n = w_{\text{magnet}} w_{K^\pm} w_{J/\psi}$, where w_{magnet} equalizes the number of events in eight settings of solenoid polarity, toroid polarity, and $B^\pm$ charge. Equalizing the contribution from each magnet polarity combination removes tracking charge asymmetries to first-order, since in one polarity a B^+ is reconstructed with the same sign of curvature as a B^- in the opposite polarity. Also equalizing the number of B^+ and B^- candidates eliminates the need to correct for different K^+ and K^- cross sections in the detector [27].

The weighted data sample contains 160360 $B^\pm$ candidates and the fit yields 89328 ± 349 $B^\pm \to J/\psi K^\pm$ decays. The $M(J/\psi K)$ invariant mass distribution for the sum of all events is shown in Fig. 1. The $M(J/\psi K)$ distribution for forward events minus backward events, incorporating asymmetry parameters from the fit, is shown in Fig. 2. Over both distributions we obtain $\chi^2/\text{ndf} = 249/214$. We measure a signal asymmetry consistent with zero: $A_{\text{FB}}(B^\pm) = [-0.24 \pm 0.41\,(\text{stat})]\%$. The asymmetry is consistent over time and with B^+ and B^- samples fitted separately. Asymmetries of the background distributions are also consistent with zero.

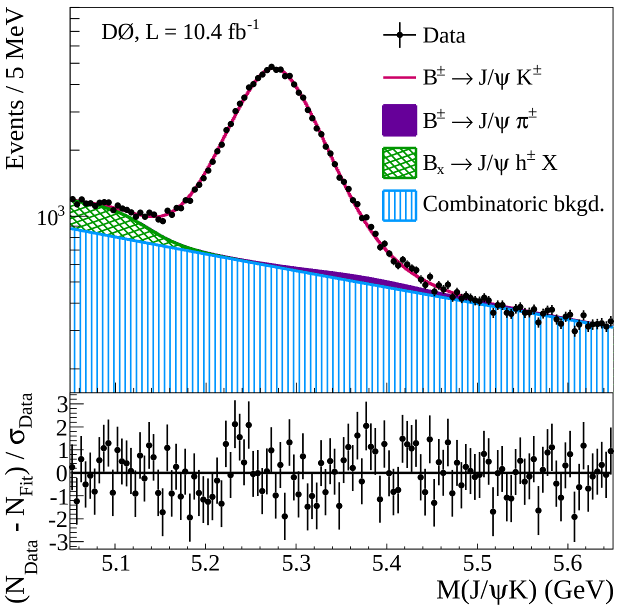

FIG. 1: (color online) Invariant mass $M(J/\psi K)$ of (forward + backward) events with fitted distributions. The lower pane shows the residuals.

To determine systematic uncertainties on $A_{\text{FB}}(B^\pm)$ a number of variations are made to the analysis. Data

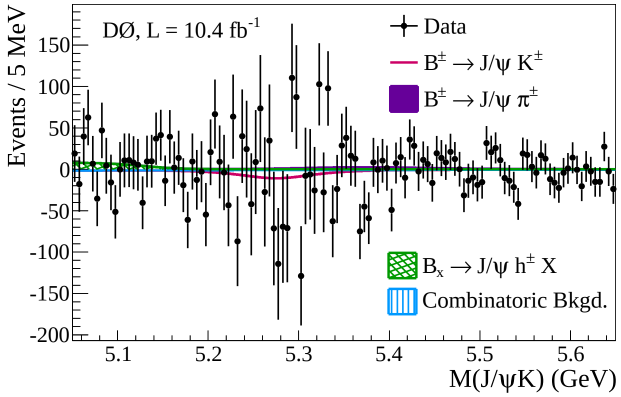

FIG. 2: (color online) Invariant mass $M(J/\psi K)$ of (forward − backward) events with fitted distributions multiplied by asymmetry parameters A_i.

sample variations include training four alternative BDTs with different variables or input samples and using a range of cuts on the BDT discriminant. Fit variations include varying the $B^\pm$ mass range, removing dependences on E_K from the fit functions, allowing the slope of $T(m_{J/\psi K})$ to float, and fixing the background asymmetry parameters to zero.

To estimate systematic error from the reconstruction asymmetries we measure $A_{\rm NS}(J/\psi)$ and $A_{\rm NS}(K^\pm)$ using alternate data samples and calculations in different bins or with alternate fit parameters. Biases in the fitting procedure are explored with ensemble tests on randomized data, comparing input and fitted values of $A_{\rm FB}(B^\pm)$. No bias is observed, and a systematic uncertainty is assigned based on the spread of results in the ensemble test. The total systematic uncertainty on the data measurement is 0.19%, as summarized in Table I.

TABLE I: Summary of uncertainties on $A_{\rm FB}(B^\pm)$ in data.

Source	Uncertainty
Statistical	0.41%
Alternative BDTs and cuts	0.17%
Fit Variations	0.06%
Reconstruction Asymmetries	0.05%
Fit Bias	0.02%
Systematic Uncertainty	0.19%
Total Uncertainty	0.45%

To compare this measurement to the SM, the MC@NLO simulation is analyzed as described above, applying $B^\pm \to J/\psi K^\pm$ selections and weights to correct for muon trigger effects. Additionally, reconstructed muon and kaon tracks must match tracks from generated $B^\pm \to J/\psi K^\pm$ decays. Since matching reconstructed $B^\pm$ candidates to generated $B^\pm$ mesons leaves no background events, $A^{\rm SM}_{\rm FB}(B^\pm)$ is calculated directly according to Eq. 1.

Systematic uncertainties on $A^{\rm SM}_{\rm FB}(B^\pm)$ are calculated by varying renormalization and factorization energy scale choices and uncertainties from the PDF set. Uncertainty on $A^{\rm SM}_{\rm FB}(B^\pm)$ due to b-quark hadronization uncertainties is not included. MC@NLO defines μ_R and μ_F for renormalization and factorization energy scales [15] as the square root of the average of $m_T^2 = m^2 + p_T^2$ for the b and $\bar{b}$ quarks [28], with b quark mass m set to 4.75 GeV. Since $A^{b\bar{b}}_{\rm FB}$ is zero at leading-order, there is a large scale dependence in predictions at next-to-leading-order [29]. Both scales are varied independently from $\frac{1}{2}\mu_{R,F}$ to $2\mu_{R,F}$ to estimate an uncertainty due to uncalculated higher orders. Half the largest spread of variations gives a systematic uncertainty of 0.44%. The negligible PDF uncertainty of 0.03% is calculated by varying the twenty CTEQ6M1 eigenvectors by their uncertainties and determining the standard deviation of the variations. We find $A^{\rm SM}_{\rm FB}(B^\pm) = [2.31 \pm 0.34\,({\rm stat}) \pm 0.44\,({\rm scale})]\%$. Combining all data and MC uncertainties in quadrature, the MC@NLO result differs from data by $(2.55 \pm 0.72)\%$, or 3.5 standard deviations.

Figure 3 shows measurements of $A_{\rm FB}(B^\pm)$ and $A^{\rm SM}_{\rm FB}(B^\pm)$ versus transverse momentum and pseudorapidity. The fully reconstructed $J/\psi K^\pm$ final state produces good kinematic agreement between reconstructed and generated $B^\pm$ mesons, so corrections to recover the true $B^\pm$ kinematics are unnecessary. The average p_T of the $B^\pm$ mesons is 12.9 GeV. We find that $A_{\rm FB}(B^\pm)$ is systematically lower than $A^{\rm SM}_{\rm FB}(B^\pm)$ for all pseudorapidities, and for $p_T(B) = 9 - 30$ GeV. Considering the MC systematic uncertainties to be correlated (uncorrelated), Fig. 3 (a) has $\chi^2 = 11.0\,(12.6)$ for three bins and Fig. 3 (b) has $\chi^2 = 6.9\,(7.3)$ for seven bins.

In conclusion, we have measured the forward-backward asymmetry in the production of $B^\pm$ mesons with $B^\pm \to J/\psi K^\pm$ decays in $p\bar{p}$ collisions at $\sqrt{s} = 1.96$ TeV. For $B^\pm$ mesons with a mean p_T of 12.9 GeV, the result is $A_{\rm FB}(B^\pm) = [-0.24 \pm 0.41\,({\rm stat}) \pm 0.19\,({\rm syst})]\%$, which is the first measurement of this quantity. The observed discrepancy of ≈ 3 standard deviations between our measurement and the MC@NLO estimate suggests that more accurate theoretical predictions are needed to interpret these results.

We thank the staffs at Fermilab and collaborating institutions, and acknowledge support from the Department of Energy and National Science Foundation (United States of America); Alternative Energies and Atomic Energy Commission and National Center for Scientific Research/National Institute of Nuclear and Particle Physics (France); Ministry of Education and Science of the Russian Federation, National Research Center “Kurchatov Institute” of the Russian Federation, and Russian Foundation for Basic Research (Russia); National Council for the Development of Science and Technology and Carlos Chagas Filho Foundation for the Support of Research in the State of Rio de Janeiro (Brazil); Department of

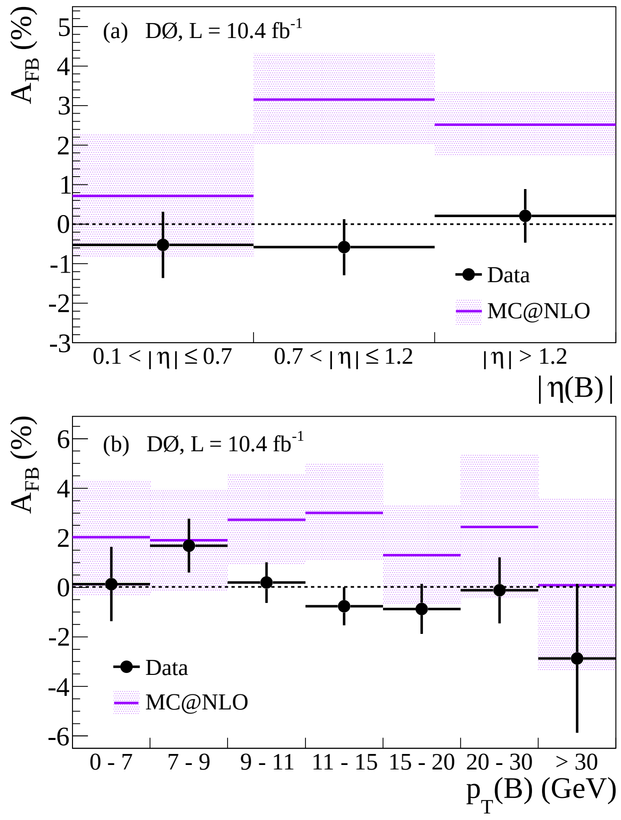

FIG. 3: (color online) Comparison of $A_{\rm FB}(B^{\pm})$ and $A_{\rm FB}^{\rm SM}(B^{\pm})$ in bins of (a) $|\eta_B|$ and (b) $p_T(B)$. Errors on data are statistical convoluted with 0.19% systematic uncertainty. Errors on MC are statistical uncertainties convoluted with systematic uncertainties.

Atomic Energy and Department of Science and Technology (India); Administrative Department of Science, Technology and Innovation (Colombia); National Council of Science and Technology (Mexico); National Research Foundation of Korea (Korea); Foundation for Fundamental Research on Matter (The Netherlands); Science and Technology Facilities Council and The Royal Society (United Kingdom); Ministry of Education, Youth and Sports (Czech Republic); Bundesministerium für Bildung und Forschung (Federal Ministry of Education and Research) and Deutsche Forschungsgemeinschaft (German Research Foundation) (Germany); Science Foundation Ireland (Ireland); Swedish Research Council (Sweden); China Academy of Sciences and National Natural Science Foundation of China (China); and Ministry of Education and Science of Ukraine (Ukraine).

[1] L.G. Almeida, G. Sterman, and W. Vogelsang, Phys. Rev. D **78**, 014008 (2008); J.H. Kühn and G. Rodrigo, J. High Energy Phys. 01 (2012) 063; J.A. Aguilar-Saavedra, D. Amidei, A. Juste, and M. Perez-Victoria, arXiv:1406.1798.

[2] V.M. Abazov *et al.* (D0 Collaboration), Phys. Rev. D **84**, 112005 (2011).

[3] T. Aaltonen *et al.* (CDF Collaboration), Phys. Rev. D **83**, 112003 (2011); Phys. Rev. D **87**, 092002 (2013); Phys. Rev. D **88**, 072003 (2013).

[4] M.I. Gresham, I.-W. Kim, and K.M. Zurek, Phys. Rev. D **83**, 114027 (2011); J.A. Aguilar-Saavedra and M. Perez-Victoria, J. High Energy Phys. 09 (2011) 097; J.F. Kamenik, J. Shu, and J. Zupan, Eur. Phys. J. C **72**, 2102 (2012).

[5] B. Grinstein and C.W. Murphy, Phys. Rev. Lett. **111**, 062003 (2013); Phys. Rev. Lett. **112**, 239901 (2014).

[6] S. Ipek, Phys. Rev. D **87**, 116010 (2013).

[7] V. M Abazov *et al.* (D0 Collaboration), Phys. Rev. D **87**, 011103(R) (2013); Phys. Rev. D **88**, 112002 (2013); Phys. Rev. D **90**, 072001 (2014); arXiv:1405.0421 (2014) (to appear in Phys. Rev. D).

[8] W. Bernreuther and Z.-G. Si, Phys. Rev. D **86**, 034026 (2012).

[9] S. Chatrchyan *et al.* (CMS Collaboration), J. High Energy Phys. 04 (2014) 191.

[10] G. Aad *et al.* (ATLAS Collaboration), J. High Energy Phys. 02 (2014) 107.

[11] R. Aaij *et al.* (LHCb Collaboration), Phys. Rev. Lett. **113**, 082003 (2014).

[12] J.H. Kühn and G. Rodrigo, Phys. Rev. D **59**, 054017 (1999).

[13] D0 defines a coordinate system with the z axis along the proton beam direction, the x axis pointing away from the Tevatron center, and the y axis pointing upwards. Pseudorapidity is defined as $\eta = -\ln[\tan(\theta/2)]$, where θ is the laboratory frame polar angle. Angle ϕ is the azimuthal angle in the x-y plane.

[14] A.V. Manohar and M. Trott, Phys. Lett. B **711**, 313 (2012).

[15] S. Frixione and B.R. Webber, J. High Energy Phys. 06 (2002) 029; S. Frixione, P. Nason, and B.R. Webber, J. High Energy Phys. 08 (2003) 007.

[16] J. Pumplin *et al.*, J. High Energy Phys. 07 (2002) 012; D. Stump *et al.*, J. High Energy Phys. 10 (2003) 046.

[17] G. Corcella, J. High Energy Phys. 01 (2001) 010.

[18] R. Brun and F. Carminati, CERN Program Library Writeup W5013, 1993. We use GEANT version 3.15.

[19] V.M. Abazov *et al.* (D0 Collaboration), Nucl. Instrum. Methods A **565**, 463 (2006).

[20] V.M. Abazov *et al.*, Nucl. Instrum. Methods A **552**, 372 (2005); V.M. Abazov *et al.* (D0 Collaboration), Nucl. Instrum. Methods A **737**, 281 (2014).

[21] Pointing angle is defined as the angle between a particle's momentum vector and the vector from the $p\bar{p}$ vertex to the particle's decay vertex, with vectors defined in the x-y plane.

[22] K.A. Olive *et al.* (Particle Data Group), Chin. Phys. C **38**, 090001 (2014).

[23] A. Hoecker *et al.*, "Toolkit for Multivariate Data Analysis", arXiv:physics/0703039v5 (2007). We use version 4.1.0.

[24] T. Sjöstrand, S. Mrenna, and P. Skands, J. High Energy Phys. 05 (2006) 026.

[25] V.M. Abazov *et al.* (D0 Collaboration), Phys. Rev. Lett. **110**, 241801 (2013).

[26] V.M. Abazov *et al.* (D0 Collaboration), Phys. Rev. D **87**,

072006 (2013).

[27] V.M. Abazov *et al.* (D0 Collaboration), Phys. Rev. D **86**, 072009 (2012); Phys. Rev. D **82**, 032001 (2010).

[28] S. Frixione (private communication).

[29] J.M. Campbell and R.K. Ellis, FERMILAB-PUB-12-078-T, arXiv:1204.1513 (2012).